Pure Appl. Chem., Vol. 77, No. 2, pp. 359–372, 2005.
DOI: 10.1351/pac200577020359

Three-dimensional modeling of inductively coupled plasma torches*

D. Bernardi, V. Colombo‡, E. Ghedini, and A. Mentrelli

Dipartimento di Ingegneria delle Costruzioni Meccaniche, Nucleari, Aeronautiche e di Metallurgia (DIEM) and Centro Interdipartimentale di Ricerca per le Applicazioni della Matematica (CIRAM), Università di Bologna, Bologna, Italy

Abstract: A 3D model for the simulation of inductively coupled plasma torches (ICPTs) working at atmospheric pressure is presented, using a customized version of the computational fluid dynamics (CFD) commercial code FLUENT®. The induction coil is taken into account in its actual 3D shape, showing the effects on the plasma discharge of removing the axisymmetric hypothesis of simplification, which characterizes 2D approaches. Steady flow and energy equations are solved for optically thin argon plasmas under the assumptions of local thermodynamic equilibrium (LTE) and laminar flow. The electromagnetic field equations are solved on an extended grid in the vector potential form. In order to evaluate the importance of various 3D effects on calculated plasma temperature and velocity fields, comparisons of our new results with the ones obtainable from 2D models and from an improved 2D model that includes 3D coil effects are presented. 3D results are shown for torches working under various geometric and operating conditions and with different coil shapes, including conventional helicoidal, as well as planar, elliptical, and double-stage configurations.

Keywords: plasma torches; plasma simulation; high-frequency; rf discharges.

INTRODUCTION

In recent years, inductively coupled plasma torches (ICPTs) have played an increasing important role in many technological processes, as a clean and effective means to produce plasma jets with high enthalpy content that can be usefully employed in a wide range of applications, such as plasma spray deposition of materials, densification and spheroidization of powders, chemical synthesis of nanoparticles, waste treatment, and others [1]. Since the success of a given process depends directly on the plasma temperature and velocity fields in the discharge and/or in the jet, which in turn depend on the geometric and operating parameters of the system, the characterization of the torch and the knowledge of the influence of such parameters on the plasma properties is of primary importance. However, the detailed diagnostics of ICPTs are very hard to perform, owing to the high temperatures involved and to the difficulty of reaching the internal zones of the device without perturbing the discharge. As an alternative, mathematical modeling represents a valid and powerful tool to predict the characteristics of this kind of system, also owing to the relevant progress recently made in computer technology, which allows for the implementation of more and more sophisticated modeling approaches. In this frame, various 2D models have been proposed in the past by different authors [2–10], to simulate the physical behavior of the plasma in ICPTs, also using an extended grid approach [5–10] for the description of the electromag-

*Paper based on a presentation at the 16th International Symposium on Plasma Chemistry (ISPC-16), Taormina, Italy, 22–27 June 2003. Other presentations are published in this issue, pp. 345–495.

‡Corresponding author

netic field. However, as all of these models assume the torch to be axisymmetric, important 3D effects owing to the actual shape of the induction coil or to the nonaxisymmetric distribution of the inlet gases, could not be revealed. Moreover, 2D models do not permit the study of torches with noncircular cross-section. A first step in trying to highlight some of the 3D effects caused by the typical helicoidal shape of the coil was the work of Xue et al. [10], which took into account within a 2D modeling also the axial component of the induction current flowing with a given inclination angle through an idealized concentric cylinder coil. In that paper, the authors showed that, although the impact on the calculated plasma temperature is negligible, some swirling effects arise in the plasma flow as a consequence of the Lorentz force induced by the axial and radial components of the electric and magnetic fields, respectively. A 3D simulation of the gas mixing in the downstream region of an ICPT was also performed by Mostaghimi et al. [11], but limiting the computational domain to a region that did not include the induction coil and its electromagnetic effects. In order to obtain a more realistic description of ICPTs, a fully 3D model [12–15], which completely removes the assumption of axisymmetry, has been recently developed. The model has been implemented in the framework of the computational fluid dynamics (CFD) commercial software FLUENT®, using a grid extending also outside the plasma region for the treatment of the electromagnetic field. A user-defined scalar (UDS) technique [9] has been adopted to suitably customize the basic FLUENT code in order to add Maxwell's equations to its built-in fluid dynamic module. In this work, simulation results obtained by means of the 3D model will be presented for different coil shapes (including conventional helicoidal as well as planar, elliptical, and double-stage configurations), torch geometries, and operating conditions and compared, when possible, to literature data or experimental observations. The calculations carried out show that the geometric parameters of the coil (such as total axial length, inclination angle of the coil turns, shape of the coil endings) play a major role in determining nonaxisymmetric behaviors of the plasma discharge which should be taken into account in the design stage of the system in order to avoid undesired effects, such as hot spot formations on the tube wall or losses at the wall of the confinement tube of material injected in the plasma.

MODELING APPROACH

Governing equations

The physical behavior of the plasma is modeled, removing the axisymmetric assumption that has been extensively used in most of the previous studies concerning ICPTs. This leads to a fully 3D model, which has been implemented in the FLUENT environment. The following assumptions have been employed:

- the flow is steady and laminar;
- the plasma is optically thin and in local thermodynamic equilibrium (LTE);
- the viscous dissipation term in the energy equation is neglected; and
- the displacement currents are neglected.

The equations for the transport of mass, momentum, and energy are written as follows:

- conservation of mass:

$$\nabla \cdot (\rho \mathbf{u}) = 0 \tag{1}$$

- conservation of momentum:

$$\nabla \cdot \left(\rho \mathbf{u}\mathbf{u}\right) = -\nabla p + \nabla \cdot \left[\mu\left(\nabla \mathbf{u} + \nabla \mathbf{u}^T\right) - \frac{2}{3}\mu \nabla \cdot \left(\mathbf{u}I\right)\right] + \rho \mathbf{g} + \mathbf{J} \times \mathbf{B} \tag{2}$$

- conservation of energy:

$$\nabla \cdot \left(\rho \mathbf{u} h\right) = \nabla \cdot \left(\frac{k}{c_{\mathrm{p}}} \nabla h \right) + \mathbf{J} \times \mathbf{E} - R \tag{3}$$

where ρ is the plasma density, p is the pressure, h is the enthalpy, T is the temperature, $\mathbf{u}$ is the velocity, k is the thermal conductivity, c_{p} is the specific heat at constant pressure, μ is the viscosity, $\mathbf{g}$ is the gravitational force, $\mathbf{E}$ is the electric field, $\mathbf{B}$ is the magnetic induction, $\mathbf{J}$ is the current density induced in the plasma, and R is the volumetric radiative loss.

The electromagnetic field generated by the current flowing in the coil ($\mathbf{J}^{\mathrm{coil}}$) and by the induced currents in the plasma ($\mathbf{J}$) can be described by means of Maxwell's equations written in their vector potential formulation:

$$\nabla^2 \mathbf{A} - i\omega\mu_{\mathrm{o}}\sigma\mathbf{A} + \mu_{\mathrm{o}}\mathbf{J}^{\mathrm{coil}} = 0 \tag{4}$$

where μ_{o} is the magnetic permeability of the free space ($4\pi \cdot 10^{-7}$ H/m), σ is the plasma electrical conductivity, and $\omega = 2\pi f$, f being the frequency of the electromagnetic field. In this work, we have used the simplified Ohm's law $\mathbf{J} = \sigma\mathbf{E}$ as suggested in [16]. The electric field $\mathbf{E}$ and the magnetic field $\mathbf{B}$ which appear in eqs. 2 and 3 are obtained from the vector potential $\mathbf{A}$ with the following expressions: $\mathbf{E} = -i\omega\mathbf{A}$, $\mathbf{B} = \nabla \times \mathbf{A}$.

Boundary conditions

Boundary conditions for the conservation equations of mass (eq. 1), momentum (eq. 2), and energy (eq. 3) are the following: on the inner wall of the confinement tube, the no-slip condition was imposed, while on the outer wall of the confinement tube a fixed temperature value of 300 K is imposed. At the torch inlet, uniform velocity profiles of gas (calculated on the basis of the given flow rates) are assumed. At the torch exit, the FLUENT outflow condition (which corresponds to a fully developed flow condition [17]) was adopted. Equation 4 is solved in a domain extending also outside the torch region, using vanishing boundary conditions for the vector potential [5,9].

Computational procedure

The governing equations for the conservation of mass (eq. 1), momentum (eq. 2) and energy (eq. 3) are solved by the FLUENT solver on an unstructured grid extending inside the torch region and the confinement tube, while the electromagnetic field equation (eq. 4) is solved by the FLUENT solver, with a UDS approach, in a domain extending also outside the torch region, in order to apply the vanishing boundary conditions for the vector potential, as previously explained in [5,9]. The computational grid is a hybrid one composed by tetrahedrons, hexahedrons, and wedges, and it is built by means of the GAMBIT® software package and then imported into the FLUENT environment. The approximate number of cells composing the grid is $4.5 \cdot 10^5$ (slightly varying depending on the torch and coil configuration). Simulations have mainly been carried out on a cluster of workstations, i.e., splitting up the grids and data in various partitions and then assigning each partition to a different compute process.

RESULTS

In the following, all the plasma fields concerning nonaxisymmetric coil shapes will refer to two perpendicular planes passing through the axis of the torch, whose relative position is evidenced by coil view, while for axisymmetric configurations, the results are presented for one of the infinite identical planes passing through the axis of the torch.

In order to test the code, numerical simulations have been performed within the 3D model for a Tekna PL-50 torch geometry (Tekna Plasma Systems, Inc.) with dimensions and operating conditions given in Fig. 1 and with the axisymmetric ring-shaped coil configuration shown in Fig. 2a. Corresponding results concerning plasma temperature and power density distributions are presented in Figs. 2b and 2c, which show a good agreement with standard 2D literature results [7,9]. As expected, the plasma fields reported in Figs. 2b and 2c are axisymmetric, as a result of the axisymmetry of both coil geometry and boundary conditions employed in the calculation.

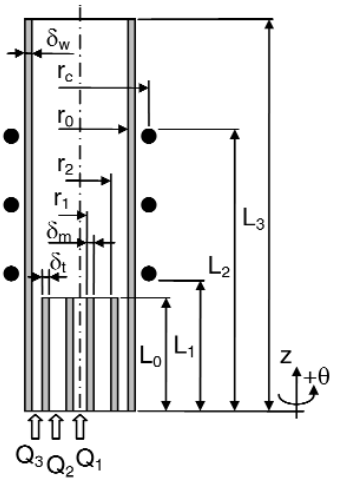

Dimensions and operating conditions	
L_0 = 50 mm	L_2 = 120 mm
L_1 = 60 mm	L_3 = 200 mm
r_0 = 25 mm	δ_w = 3.5 mm
r_1 =1.5 mm	δ_m = 2.0 mm
r_2 = 18.8 mm	δ_t = 2.2 mm
r_c = 33 mm	d_c = 6 mm
Q_1 = 1 slpm	Q_3 = 31 slpm
Q_2 = 3 slpm	
P = 5 kW	f = 3 MHz

Fig. 1 Tekna PL-50 plasma torch geometry.

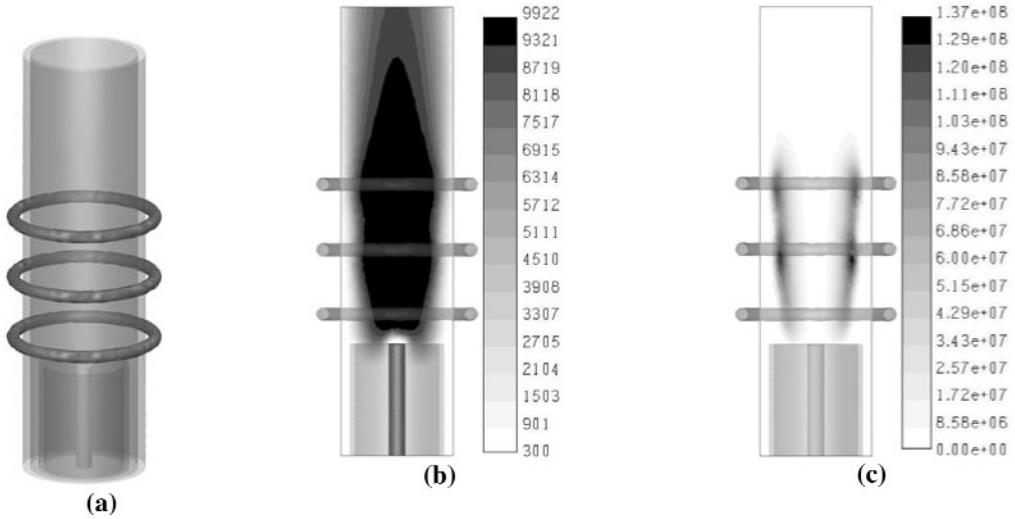

Fig. 2 ***Test case: axisymmetric ring-shaped coil.*** (a) Schematic of the confinement tube and induction coil; (b) plasma temperature field [K]; (c) power dissipation [W/m^3].

In Fig. 3, another test case is considered for a torch configuration with the same dimensions and working conditions of Fig. 1, but with an idealized cylindrical coil in which the electric current flows with an inclination angle of 3.70° with respect to the horizontal plane (Fig. 3a). For this case, results obtained by means of the 3D model are presented in Figs. 3b, 3c, and 3d, showing plasma temperature, power density, and tangential velocity fields, respectively. These data can be qualitatively compared to

the ones obtained by Xue et al. [10] in the frame of an improved 2D model, taking into account also the axial coil current component, for the same torch geometry and working conditions, but for a discharge power of 25 kW. In particular, Fig. 3d shows that a swirl velocity component arises due to the tangential Lorentz force generated by the axial component of the coil current, according to the results presented in [10]. Plasma temperature and power density distributions of Figs. 3b and 3c differ from the ones of Fig. 2 mainly due to the coil shape.

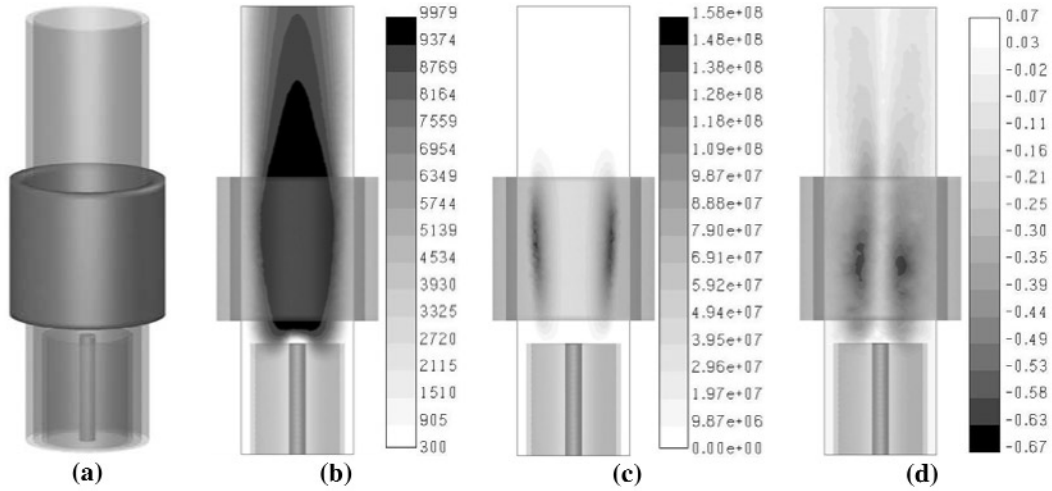

Fig. 3 ***Test case: axisymmetric cylindrical coil.*** (a) Schematic of the confinement tube and induction coil; (b) plasma temperature field [K]; (c) power dissipation [W/m^3]; (d) tangential velocity [m/s].

A more realistic coil configuration with 2.5 turns inclined of 6.60° with respect to the horizontal plane, is taken into account in Fig. 4a, for a torch with the same dimensions and operating conditions of Fig. 1. In this case, the strong nonaxisymmetry of the coil leads to a significant displacement of the plasma discharge and to the formation of a hot spot in the confinement tube. This behavior is due to the unbalancing of the Lorentz forces in the radial direction, which overcome in magnitude the tangential Lorentz forces due to the axial component of the coil current, the main source of nonaxisymmetry being the coil shape and not the axial current component. The formation of a hot spot in the confinement tube makes this coil configuration unsuitable for technological applications because of the risk of damaging the tube wall in the absence of a swirl component for the sheath gas.

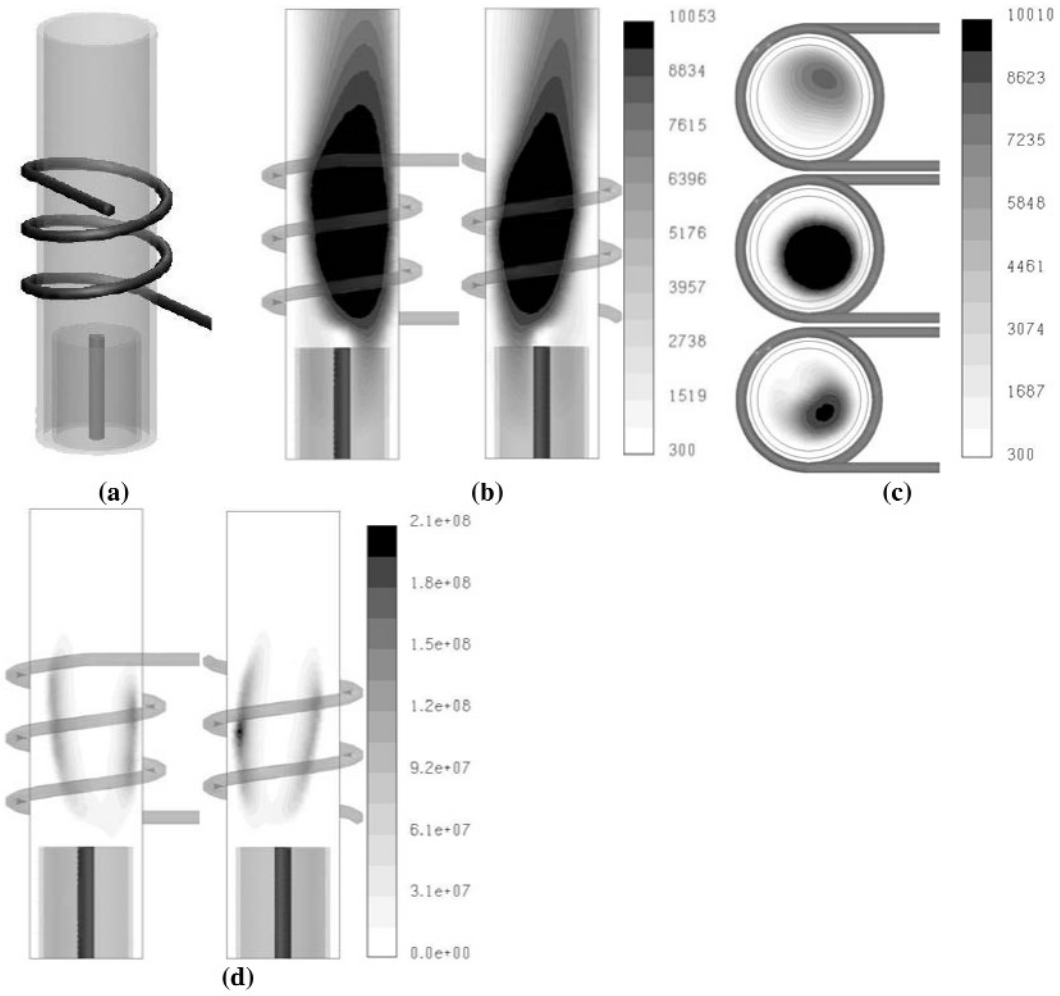

Fig. 4 ***2.5 turns coil.*** (a) Schematic of the confinement tube and induction coil; (b) plasma temperature fields [K]; (c) plasma and wall temperature fields [K] on three horizontal planes located at z = 60, 92, 200 mm, respectively, from bottom to top; (d) power dissipation [W/m^3].

In Fig. 5, results concerning a coil configuration with 5 turns inclined of 3.68° with respect to the horizontal plane are presented, for a discharge power of 25 kW. Torch dimensions and working parameters that differ from those reported in Fig. 1 are summarized in Fig. 5a. Plasma temperature fields reported in Figs. 5b and 5c show the more axisymmetric behavior of the plasma discharge with respect to the 2.5 turns coil configuration, while Fig. 5d shows the arising of a swirl velocity component of greater order of magnitude than that obtained with the idealized cylindrical coil (Fig. 3d). It is worth noting that, also in this case, the absence of a swirl component in the sheath gas may lead to undesired hot spots in the confinement tube.

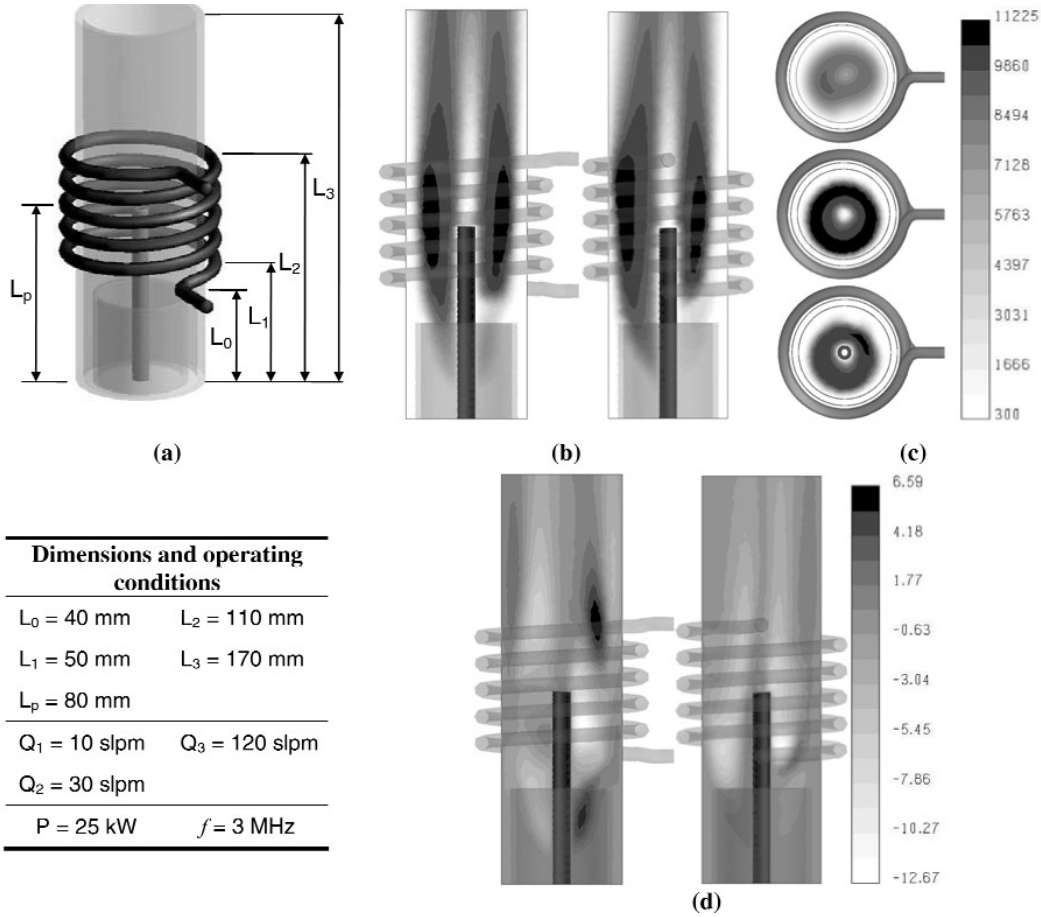

Dimensions and operating conditions	
L_0 = 40 mm	L_2 = 110 mm
L_1 = 50 mm	L_3 = 170 mm
L_p = 80 mm	
Q_1 = 10 slpm	Q_3 = 120 slpm
Q_2 = 30 slpm	
P = 25 kW	f = 3 MHz

Fig. 5 ***5 turns coil.*** (a) Schematic of the confinement tube and induction coil; (b) plasma temperature fields [K]; (c) plasma and wall temperature fields [K] on three horizontal planes located at z = 60, 90, 170 mm, respectively, from bottom to top; (d) tangential velocity component [m/s].

The effects of introducing an inlet swirl velocity component in the sheath gas (of magnitude +20 and –20 m/s, assuming the positive orientation of the θ-coordinate as indicated in Fig. 1) for the case of Fig. 5 are shown in Fig. 6. Plasma temperature fields presented in Figs. 6a and 6b show that the discharge is now better confined and that the hot plasma regions are located at greater distance from the tube wall than in the case without inlet swirl component. Moreover, a comparison of the results reported in Figs. 6a and 6b leads to the conclusion that reversing the orientation of the inlet swirl component induces sensible changes in the discharge shape, and not just an inversion of the tangential velocity of the gas as would be the case of an axisymmetric coil configuration. The effects of nonaxisymmetric behavior of the discharge are also visible in the temperature fields at the exit of the torch for the two different orientations of the swirl gas, as shown in Fig. 6c.

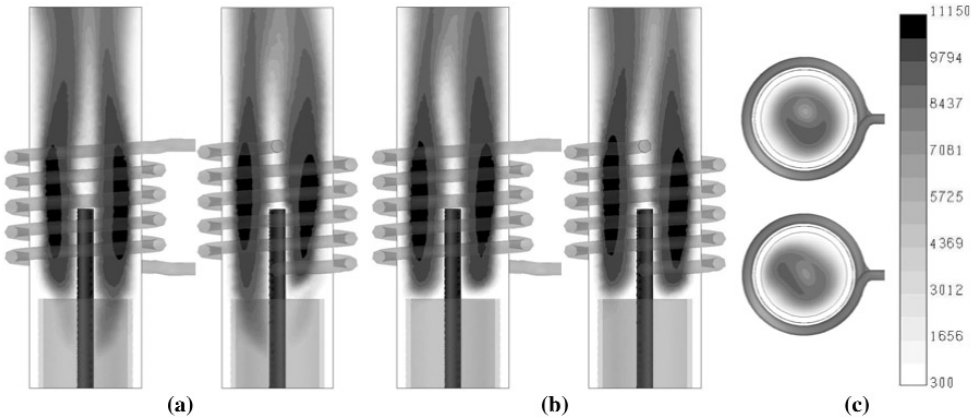

Fig. 6 ***5 turns coil with swirl gas.*** (a) plasma temperature fields [K] for $v_\theta = 20$ m/s; (b) plasma temperature fields [K] for $v_\theta = -20$ m/s; (c) plasma and wall temperature fields [K] at the torch exit for the case (a) and (b), respectively, from bottom to top.

In Fig. 7, results are shown for a torch [18] designed for applications in atmospheric plasma spraying of materials, which is here supposed to operate at a discharge power level of 6 kW. The slight nonaxisymmetry of the calculated plasma temperature field, which is mainly located in the regions cor-

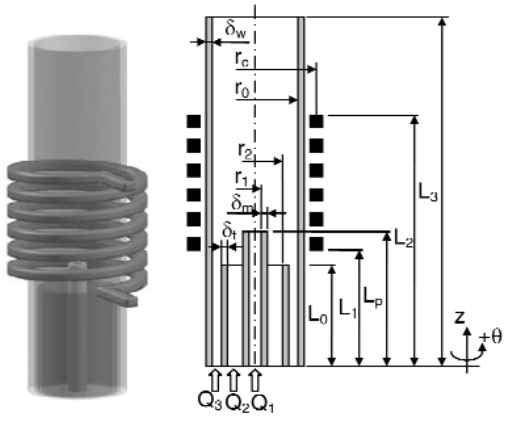

Dimensions and operating conditions	
L_0 = 45 mm	L_2 = 100 mm
L_1 = 55 mm	L_3 = 150 mm
r_0 = 13.5 mm	δ_w = 2 mm
r_1 = 1.5 mm	δ_m = 1.5 mm
r_2 = 11 mm	δ_t = 1.5 mm
r_c = mm	d_c = mm
Q_1 = 2 slpm	Q_3 = 33.3 slpm
Q_2 = 6.7 slpm	v_0 = 10 m/s
P = 6 kW	f = 3.7 MHz

(b)

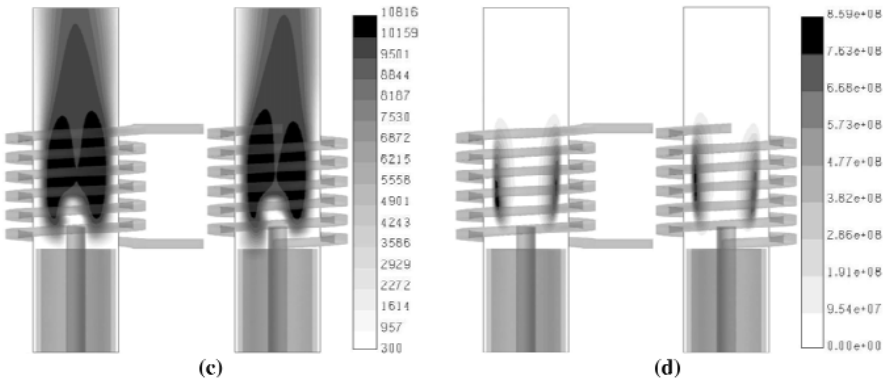

Fig. 7 ***Plasma spraying torch.*** (a) Schematic of the confinement tube and induction coil; (b) dimensions and operating conditions; (c) plasma temperature fields [K]; (d) power dissipation [W/m^3].

responding to the first and last turns of the coil, as shown in Fig. 7c, is in qualitative good agreement with the experimental measurements carried out in [18] by means of an enthalpy probe technique. Since there are many parameters affecting the spraying process both on the powder side (such as powder type, size, injection position) and on the plasma side (such as operating power, flow rates, gas type, coil shape), 3D modeling can be a useful tool in the design of such systems.

Another example of 3D modeling applied to a real torch, which was designed to be used in plasma-assisted chemical synthesis and deposition of pure silica [5,6], is shown in Fig. 8. In this application, the main objective was to reduce nonaxisymmetry effects in plasma temperature distribution by means of a quite unconventional axial extension (12 turns) of the induction coil. The numerical results actually seem to confirm that the plasma temperature and power density distributions in this system (Figs. 8c and 8d) are characterized by a very high degree of axisymmetry.

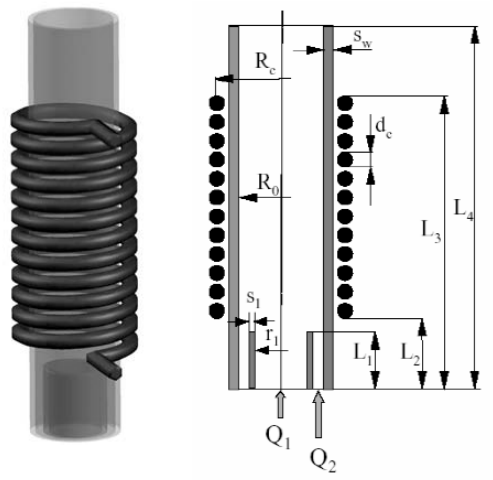

Dimensions and operating conditions	
r_1 = 10 mm	R_0 = 15 mm
s_1 = 2 mm	s_w = 2 mm
R_c = 21 mm	d_c = 6 mm
L_1= 25 mm	L_3 = 125 mm
L_2 = 30 mm	L_4 = 160 mm
Q_1 = 0.1 slpm	Q_2 = 1 slpm
P = 1.2 kW	f = 13.56 MHz

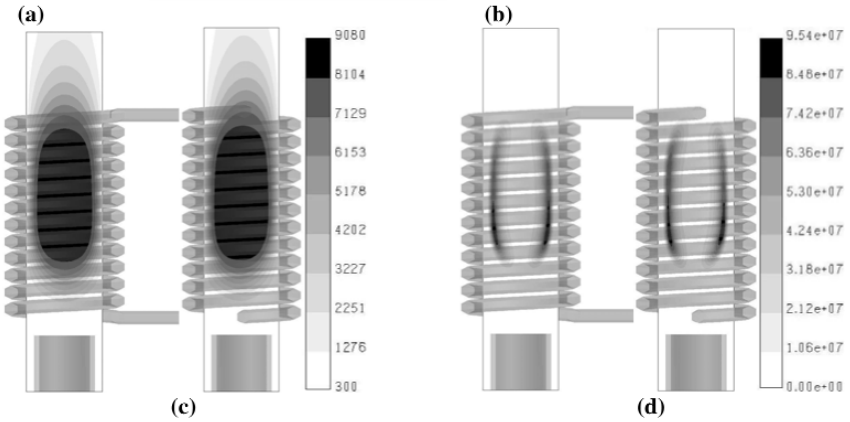

Fig. 8 ***Silica deposition torch.*** (a) Schematic of the confinement tube and induction coil; (b) dimensions and operating conditions; (c) plasma temperature fields [K]; (d) power dissipation [W/m^3].

As further examples, Figs. 9–11 show some selected results concerning nonstandard coil and confinement tube configurations for which the 3D code could help as a powerful tool for the characterization of the discharge. In Fig. 9, a torch with an elliptical-shaped confinement tube, which might be useful to generate plasma jets for large area applications, is presented. Corresponding plasma temperature fields calculated within the 3D model are reported in Fig. 9b, showing that the nonaxisymmetry of the discharge is mainly located on the plane passing through the minor axis of the elliptical cross-section

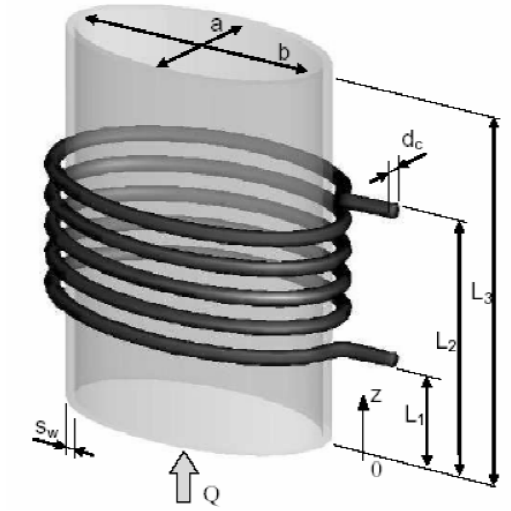

Dimensions and operating conditions	
a = 50 mm	d_c = 6 mm
b = 100 mm	s_w = 3.5 mm
L_1 = 37 mm	L_3 = 150 mm
L_2 = 103 mm	Q = 40 slpm
P = 5 kW	f = 3 MHz

(a)

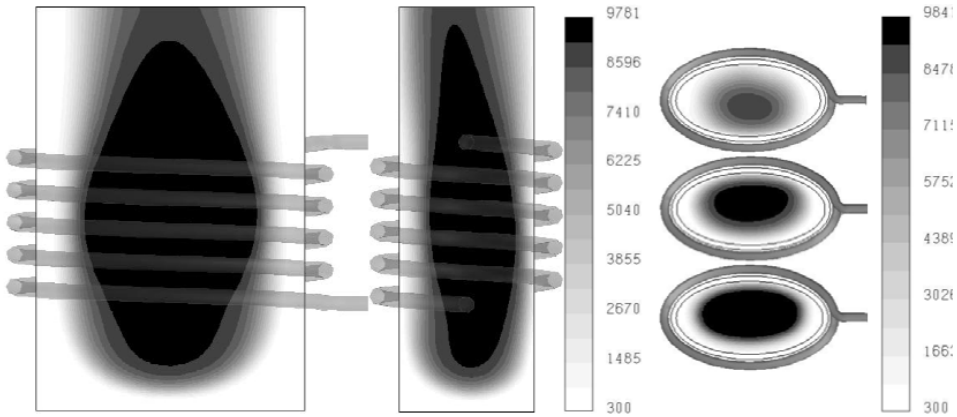

(b) (c)

Fig. 9 ***Elliptical torch*.** (a) Schematic of the confinement tube and induction coil with dimensions and operating conditions; (b) plasma temperature fields [K]; (c) plasma and wall temperature fields [K] on three horizontal planes located at z = 40, 70, 150 mm, respectively, from bottom to top.

of the torch. This effect is also evidenced by the temperature fields on different horizontal planes, shown in Fig. 9c. In Fig. 10, a planar coil configuration is taken into account, as suggested in [19], in order to improve the fluid dynamic characteristics of the plasma gas for the optimization of the chemical processes inside the torch, avoiding material deposition on the tube wall. Finally, Fig. 11 shows some 3D simulation results for a double-stage torch, first introduced by McKelliget [19] and than studied by some of the authors in [20–23] within a 2D model. This configuration reveals some interesting features, such as the possibility of working with high gas flow rates and of having long residence times in a high-temperature plasma region for the injected particles (owing to the axially extended discharge, as shown in Fig. 11c) in order to obtain their complete melting.

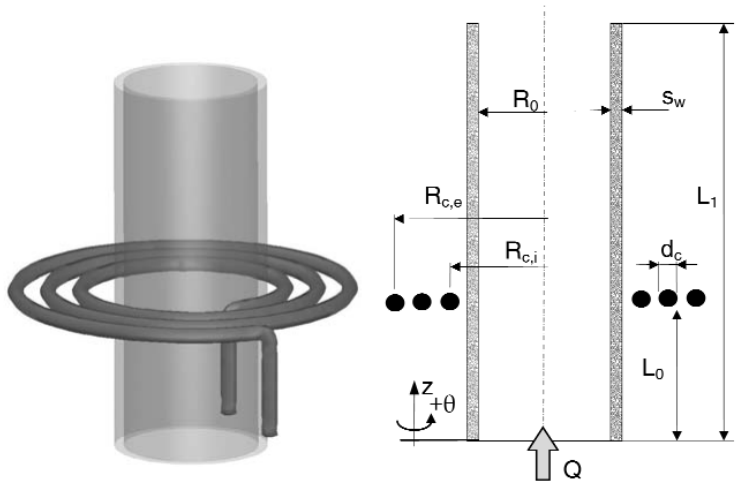

Dimensions and operating conditions	
R_0 = 25 mm	$R_{c,i}$ = 33 mm
s_w = 3.5 mm	$R_{c,e}$ = 70 mm
L_0 = 57 mm	d_c = 6 mm
L_1 = 140 mm	Q = 35 slpm
P = 5 kW	f = 3 MHz

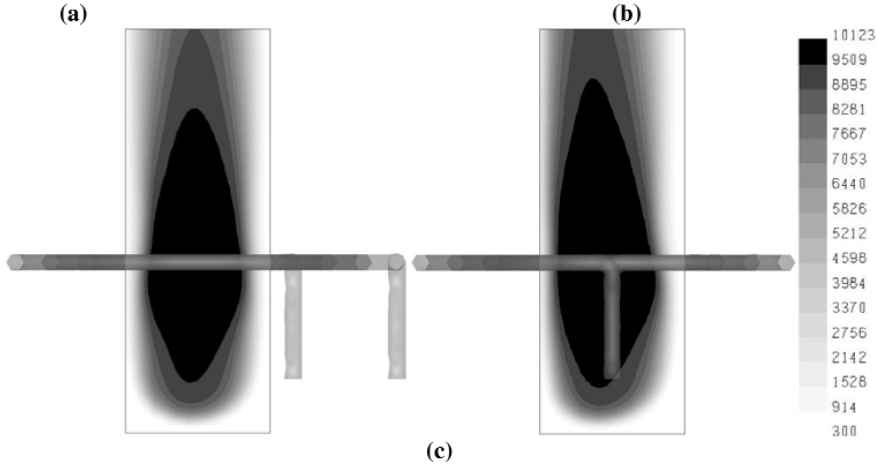

Fig. 10 ***Planar coil torch.*** (a) Schematic of the confinement tube; (b) induction coil with dimensions and operating conditions; (c) plasma temperature fields [K].

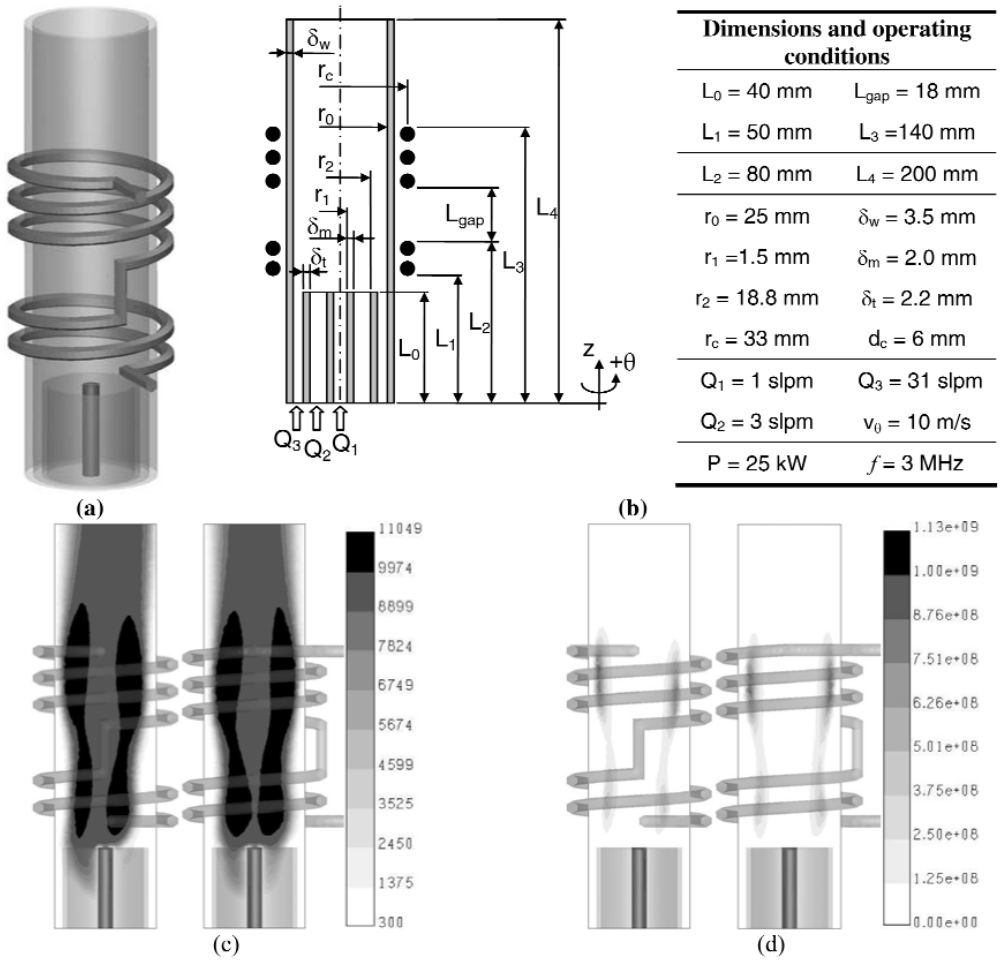

Dimensions and operating conditions	
L_0 = 40 mm	L_{gap} = 18 mm
L_1 = 50 mm	L_3 =140 mm
L_2 = 80 mm	L_4 = 200 mm
r_0 = 25 mm	δ_w = 3.5 mm
r_1 =1.5 mm	δ_m = 2.0 mm
r_2 = 18.8 mm	δ_t = 2.2 mm
r_c = 33 mm	d_c = 6 mm
Q_1 = 1 slpm	Q_3 = 31 slpm
Q_2 = 3 slpm	v_{θ} = 10 m/s
P = 25 kW	f = 3 MHz

Fig. 11 ***Double-stage RF–RF torch.*** (a) Schematic of the confinement tube and induction coil; (b) dimensions and operating conditions; (c) plasma temperature fields [K]; (d) power dissipation [W/m^3].

CONCLUSIONS

The results presented in this paper show that 3D effects may arise in the ICPT's discharge depending mainly on the coil shape and play an important role in the physical characterization of this kind of devices. When only the axial component of induction coil current is taken into account, within an axisymmetric coil configuration, the effects on plasma temperature distribution are negligible, while most important effects on nonaxisymmetry arise when the real induction coil shape is considered. The main feature of 3D modeling in ICPTs is the possibility of taking into account nonstandard coil and confinement tube shapes in the design stage of this kind of device for a particular application, in order to optimize the discharge characteristics, since the complexity of the phenomena involved inside this kind of device, especially for what concerns the fluid dynamics, let the results be quite difficult to foresee when changing torch operating parameters. For this reason, the 3D code can be a useful tool in the design of ICPTs. For example, in plasma treatment of powders, it is possible to determine the coil shape influence on temperature and velocity fields in the design stage of the process, in order to maximize the quality of the results (e.g., coating properties, ratio of spheroidization, and all of the parameters that depend upon the thermal history of the particles inside the plasma) and avoiding powder deposition on the

confinement tube wall. The next step in this research will be the setting up of a series of comparisons between numerical and experimental results for different torch operating conditions and geometries, in order to test and tune the code [24].

ACKNOWLEDGMENTS

This work was performed with partial financial support from the University of Bologna Goal-Oriented project 2001–2003 and ex-60% 2001–2002 projects, from the Italian Ministry of Education, University and Scientific Research (M.I.U.R.) national project COFIN-2002 and from the National Group for Mathematical Physics (G.N.F.M.) of the Italian Institute of High Mathematics.

REFERENCES

1. M. I. Boulos. *High Temp. Mater. Proc.* **1** (1), 17–39 (1997).
2. J. Mostaghimi and M. I. Boulos. *Plasma Chem. Plasma Process*. **9** (1), 25–44 (1989).
3. X. Chen and E. Pfender. *Plasma Chem. Plasma Process.* **11** (1), 103 (1991).
4. P. Proulx, J. Mostaghimi, M. I. Boulos. *Int. J. Heat Mass Transfer* **34** (10), 2571–2579 (1991).
5. V. Colombo, C. Panciatichi, A. Zazo, G. Cocito, L. Cognolato. *IEEE Trans. Plasma Sci.* **25** (5), 1073–1080 (1997).
6. C. Panciatichi, P. Cocito, M. C. N. De Leo. "Vitreous silica layers Synthesized by an inductively coupled plasma torch (ICPT) working at atmospheric pressure: Deposition and characterization", in *Progress in Plasma Processing of Materials 1999*, P. Fauchais and J. Amoroux (Eds.), pp. 885–890, Begell House, New York (1999).
7. S. Xue, P. Proulx, M. I. Boulos. *J. Phys. D: Appl. Phys.* **34** (12), 1897–1906 (2001).
8. M. I. Boulos. *J. Visualization* **4** (1), 19–28 (2001).
9. D. Bernardi, V. Colombo, E. Ghedini, A. Mentrelli. *Eur. Phys. J. D* **27**, 55–72 (2003).
10. S. Xue, P. Proulx, M. I. Boulos. *Plasma Chem. Plasma Process.* **23** (2), 245–263 (2002).
11. Z. Njah, J. Mostaghimi, M. Boulos. *Int. J. Heat Mass Transfer* **36** (16), 3909–3919 (1993).
12. D. Bernardi, V. Colombo, E. Ghedini, A. Mentrelli. *Eur. Phys. J. D* **22** (1), 119–125 (2003).
13. D. Bernardi, V. Colombo, E. Ghedini, A. Mentrelli. *Eur. Phys. J. D* **25** (3), 271–277 (2003).
14. D. Bernardi, V. Colombo, E. Ghedini, A. Mentrelli. *Eur. Phys. J. D* **25** (3), 279–285 (2003).
15. D. Bernardi, V. Colombo, E. Ghedini, A. Mentrelli. "Three-dimensional effects in the design of inductively coupled plasma torches", in *Atti del XVI Congresso dell'Associazione Italiana del Vuoto*, pp. 267–272, Editrice Compositori, Bologna (2003).
16. M. Mitchner and C. H. Krueger. *Partially Ionized Gases*, John Wiley, New York (1973).
17. *FLUENT© 6.1 User's Guide*, Fluent Inc., Lebanon, NH (2003).
18. G. Nutsch. "Atmospheric induction plasma spraying", in *Progress in Plasma Processing of Materials 2003*, P. Fauchais (Ed.), pp. 401–408, Begell House, New York (2003).
19. J. W. McKelliget and N. El-Kaddah. *J. Appl. Phys.* **64** (6), 2948 (1988).
20. D. Bernardi, V. Colombo, G. G. M. Coppa, E. Ghedini, A. Mentrelli. "Numerical modelling of RF-RF hybrid plasma torches and parametric study for various geometric, flow and electric configurations", in *Progress in Plasma Processing of Materials 2001*, P. Fauchais (Ed.), pp. 339–346, Begell House, New York (2001).
21. D. Bernardi, V. Colombo, G. G. M. Coppa, E. Ghedini, A. Mentrelli. "Investigation on operating conditions and efficiency optimization of RF-RF hybrid plasma torches", in *Progress in Plasma Processing of Materials 2001*, P. Fauchais (Ed.), pp. 359–364, Begell House, New York (2001).
22. D. Bernardi, V. Colombo, G. G. M. Coppa, E. Ghedini, A. Mentrelli. *High Temp. Mater. Proc.* **7** (1), 71–76 (2003).

23. D. Bernardi, V. Colombo, E. Ghedini, A. Mentrelli. *Eur. Phys. J. D* **28** (3), 399–422 (2004).
24. V. Colombo, G. Gao, E. Ghedini, J. Mostaghimi. "Asymmetry effects in the diagnostics and simulation of RF inductively coupled plasma torch", in *Proceedings of the 16th International Symposium on Plasma Chemistry (ISPC-16)*, on CD-ROM (2003).